13th World Conference on Earthquake Engineering
Vancouver, B.C., Canada
August 1-6, 2004
Paper No. 119

PREDICTION OF FAULT RUPTURE PROPAGATION BASED ON PHISICAL MODEL TESTS IN SANDY SOIL DEPOSIT

Jea Woo LEE[1], Masanori HAMADA[2] , Go TABUCHI[3] and Kazuhito SUZUKI[4]

SUMMARY

This paper presents the results of experimental studies to examine propagation of fault ruptures with particular concern on dip-slip fault. Based on the results from fault box tests under 1-g and centrifuge condition, the pattern of rupture propagation through a sandy soil and the location of surface rupture were investigated. The variation of dip angle and soil density appeared as major affecting factors to form the pattern of rupture propagation. The distortion and subsidence of surface ground have been examined as well. Accordingly, it is confirmed that reproduction of fault rupture propagation in sandy soil deposit using physical model could be largely affected by its confining stresses from this research.

INTRODUCTION

Two large scaled earthquakes occurred at Kocaeli (Mw 7.3, 1999, Turkey) and Jiji (Mw 7.9, 1999, Taiwan) have definitely revealed that surface fault failures could cause severe damages to buildings and major infrastructures located within the zone of faulting. Generally the damages induced by surface rupture are considered as being due to discontinuous deformations of overlying soil resulting in vertical or lateral offset at the surface of soil. **Figure 1** shows the discontinuous deformation through an overlying ground due to reverse fault that produces the distinct fault rupture plane and the scarp on the ground surface. Furthermore, as shown in **Figure 1,** the rupture propagation can accompany the distortion of ground surface depending upon the ductility of the material overlying the active fault as well.

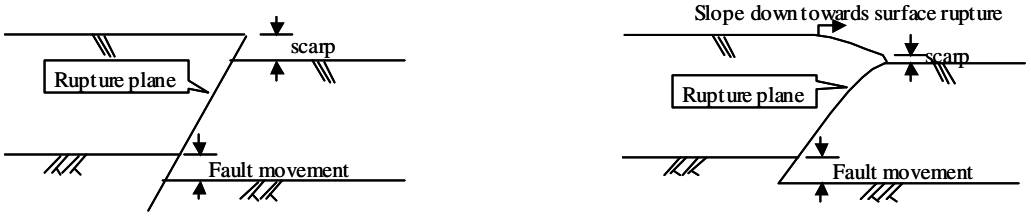

(a) Brittle material; stiff clay and rock mass

(b) Ductile material; sand and soft clay

Figure 1 Earthquake fault rupture due to reverse fault

One of the most efficient ways to mitigate the damages from the phenomenon is to avoid construction

[1]Ph.D. Candidate, Waseda University, Tokyo, Japan. Email:jay-lee@aoni.waseda.jp
[2]Professor, Waseda University, Tokyo, Japan. Email:hamada@waseda.jp
[3]Technician, JAXA, Tokyo, Japan.
[4]Graduate student, Waseda University, Tokyo, Japan.

of structures near the risky zone. For that purpose the first step should be to find out the exact location of potential earthquake surface fault rupture. This circumstance led most of the previous researches (Cole et al. [1]; Bray et al. [2]; Tani et al. [3], Ueta et al. [4]) relating to this subject to mainly concentrate on the grasp of location of surface rupture and required offset of bedrock to rupture the surface. Only a limited number of researches mainly concerning the location of surface rupture in a sandy soil (Cole et al. [1]; Tani et al. [3], Ueta et al. [4]) have been conducted based on small-scale physical models so far. However, those experimental studies seem to be conducted under extremely low level of confining stresses, which may yield somewhat different trends from the actual behavior considering the thickness of deformable soil layers in real field.

On the other hand, Roth et al. [5] performed a series of centrifugal tests to estimate the effect of faulting speed on the pattern of rupture propagation in dry sand. Stone et al. [6] showed the formation of localized shearing deformations within a sandy soil mass on a centrifuge at 100g. But these models hardly mentioned about the location of surface rupture and the distortion of model surface induced by the fault movements at bedrock.

Meanwhile, unlike the individual structures such as buildings for residence which occupied merely a limited area, the lifeline facilities such as water supply, gas pipeline and traffic tunnels are difficult to be designed to avoid the risky zone due to their broad ranges. This fact introduces the allowance of constructing structures on or in the ground near active faults with sufficient consideration for the countermeasures against the damages from the surface fault rupture. In order to establish the task, the shape and extent of deformed ground surface as well as the location of surface fault rupture should be estimated especially for the sandy soils which tends to exhibit angular distortion of the ground surface prior to reaching of shear rupture plane to the ground surface and occurrence of the scarp on the ground surface.

In this study a series of physical model tests under both 1-g and centrifuge conditions has been carried out to examine the rupture propagation in dry sand with particular concern on dip slip fault. The effects of inclination of fault plane and fault types have been examined through the 1-g fault tests with the dry sands having two different relative densities. In particular the rupture patterns for reverse fault have been investigated through comparison among the testing results under various gravitational conditions. These tests show that the location of the surface rupture in a sandy soil mass using the physical model under 1-g condition can be largely affected by the thickness of model itself. It is thus found that the prediction of location of surface rupture based on the results from 1-g tests should be meaningfully verified with those from centrifuge tests.

SETUP AND PROCEDURE FOR FAULT RUPTURE TESTS

Preparation of Testing Apparatus

Two kinds of testing devices have been used for the dip-slip faulting tests under 1-g and centrifuge condition in this study.

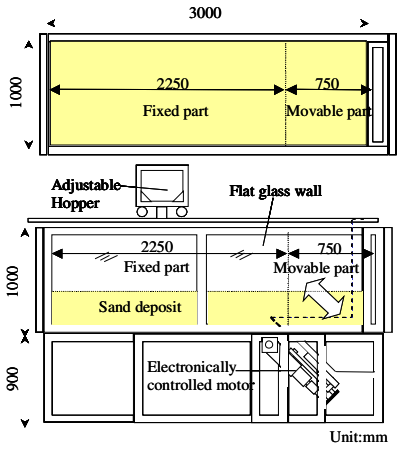

Figure 2 Schematic drawing of Apparatus Ⅰ

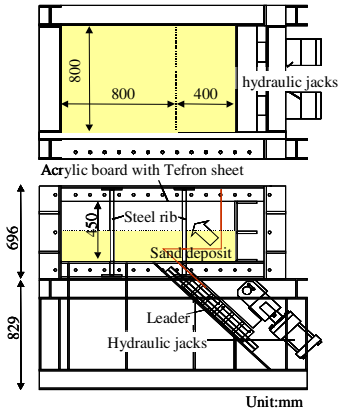

Figure.3 Schematic drawing of Apparatus Ⅱ

The device for 1-g test (Apparatus I, **Figure 2**) was built up with steel frame and glass-walled box of which the dimension is 2.0m, 0.5m, 1.0m in length, width and depth. A part of basal plate and end wall in the testing box could be moved up or down along various angles with respect to the fixed base using an electronically controlled high-capacity motor. Three sets of interchangeable angles (30°, 45°, 60°) were utilized to make it possible to examine the effect of the fault dip angle on the propagation of fault rupture. The adjustable rolling hopper was also assembled to deposit the dry sand in the testing box at a uniform density. By changing the mesh size of steel net at the outlet of the hopper, the quantity of dropping sand from the outlet can be adjusted to make the targeted density of the deposited sand.

The testing apparatus for centrifuge tests (Apparatus II, **Figure 3**), was constructed with a steel frame consisted of 30mm thick steel plates and an acrylic board with thickness of 50mm on one side of the box through which the behavior of ground model could be observed during an experiment. The dimension of the apparatus is 1.2m, 0.8m, 0.45m in length, width and depth. Similarly as 1-g tests, a part of the testing box could be moved up along a fixed dip angle (45° in this study) relative to the fixed part using double 200tonf-capacity hydraulic jacks. The apparatus were also equipped with the earth pressure cells and the remote-control video camera as shown in **Figure 4** to observe the deformation of surface of ground model and the change of earth pressures at the bottom of the ground model. To minimize the frictional resistance between the soil specimen and the each sidewall of apparatus during the tests, Teflon sheet that show sufficiently small friction on its surface was attached on each inner side of wall prior to the placement of sand.

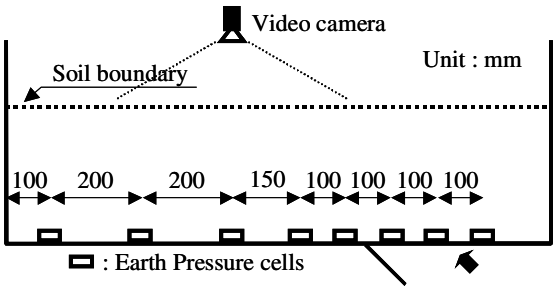

Figure 4 Layout of Video camera and Earth pressure cells in centrifuge testing box

Testing Procedure

The procedure for each test under 1-g condition is summarized as bellows;

i) Preparation of uniform sand layer using hopper with placement of a black sand layer and targets at every 3~5 ㎝ in thickness, ii) Activation of up or down movement of the movable part in the testing box to every incremental displacement with constant speed of 2mm/min., iii) Taking photos of both sides of deformed specimen and surface of soil mass at each increment of vertical displacement, iv) Repetition of processes described as ii) and iii) to the overall required vertical movement to make the fault rupture reach to the model surface, v) Then, finally sketching the shape of surface rupture and measuring the location of rupture on surface.

Meanwhile, the tests under centrifuge condition were essentially processed according to the same procedure for the 1-g test as described above.

Specimen for Test

The silica No. 7 was commonly used in both of the 1-g tests and the centrifuge tests. As for the 1g-tests, the effect of soil density was examined, but for the centrifuge tests, only a dense sand was included as the specimen for the tests The parameters related to soil deposit are summarized in **Table 1**.

TABLE 1: Soil parameters used in tests

Material Type	Silica Sand No. 7
Average Grain size (D_{50})	0.157mm
Uniformity Coeff. (U_c)	1.55
Relative Density (D_r)	Loose : 59±4%(1-g) Dense : 83±4%(1-g), 74±6.58%(centrifuge)
Dry density (γ)	1.401tonf/㎥≤ γ ≤1.452tonf/㎥

Testing Cases

Totally 36 cases of experiments under 1-g condition were conducted with variation of the thickness of ground model and the dip angle.. And further careful consideration on the effects of confining pressures relating to the model thickness was taken into the centrifuge models in which the results from four cases with a fixed dip angle (45°) accounted for those effects in terms of the equivalent thickness of ground model at a given gravity. All testing cases are summarized in **Table 2**.

TABLE 2:Testing Cases for 1-g fault box tests

Type of Fault	1-g test		Centrifuge test
	Reverse fault	Normal fault	Reverse fault only
Dip angle of fault (θ)	30°, 45°, 60° (H=20 ㎝)	30°, 45°, 60° (H=20 ㎝)	45°
Thickness of ground model (H)	10 ㎝, 15 ㎝, 20 ㎝, 25 ㎝, 30 ㎝, 40 ㎝, 60 ㎝	20 ㎝	20 ㎝ × 20G = 4.0m 20 ㎝ × 30G = 6.0m 15 ㎝ × 50G = 7.5m 30 ㎝ × 30G = 9.0m

OBSERVED BEHAVIOR FROM 1-G MODEL TESTS

Rupture pattern from 1-g Models

The typical patterns of propagation of fault rupture through a dry sand deposit are shown in the photographs shown in **Figure 5**. The rupture plane for reverse fault tended to gradually decrease in dip near the surface of ground and finally reached to the ground surface farer than the extension of fault plane with respect to the distance from the bedrock fault. Most of them appeared in the plural number of failure planes as shown in **Figure 5 (a)**. Particularly the larger the thickness of ground model was, the more the number of failure planes developed. In addition, as for reverse fault, the differential displacement at bedrock fault tended to propagate to the ground surface spreading out over a wide zone rather than proceeding upward along a straight line which might be expected to come into view at ultimately brittle material. Accordingly this spreading of differential displacement formed the deformation of surface ground expressed by warping that is called “flexure” as shown in **Figure 5 (a)**. On the contrary, normal faults were seen to produce rather distinct failure planes, all of which increased in dip as they approached the ground surface. For normal fault the differential displacement at bedrock tended to create a group of three singular failure planes, each of which was generated sequentially as shown in **Figure 5 (b)**. The failure planes numbered by ① and ② in **Figure 5 (b)** first took place at early stage of normal fault. As the fault movement at bedrock continued, the third failure plane numbered by ③in **Figure 5 (b)** was produced in the part of hanging wall. Some cases showed skip of generation of the failure plane ②. These successively developed failure planes formed a subsided area surrounded by the second and third failure planes, which is called “graben”.

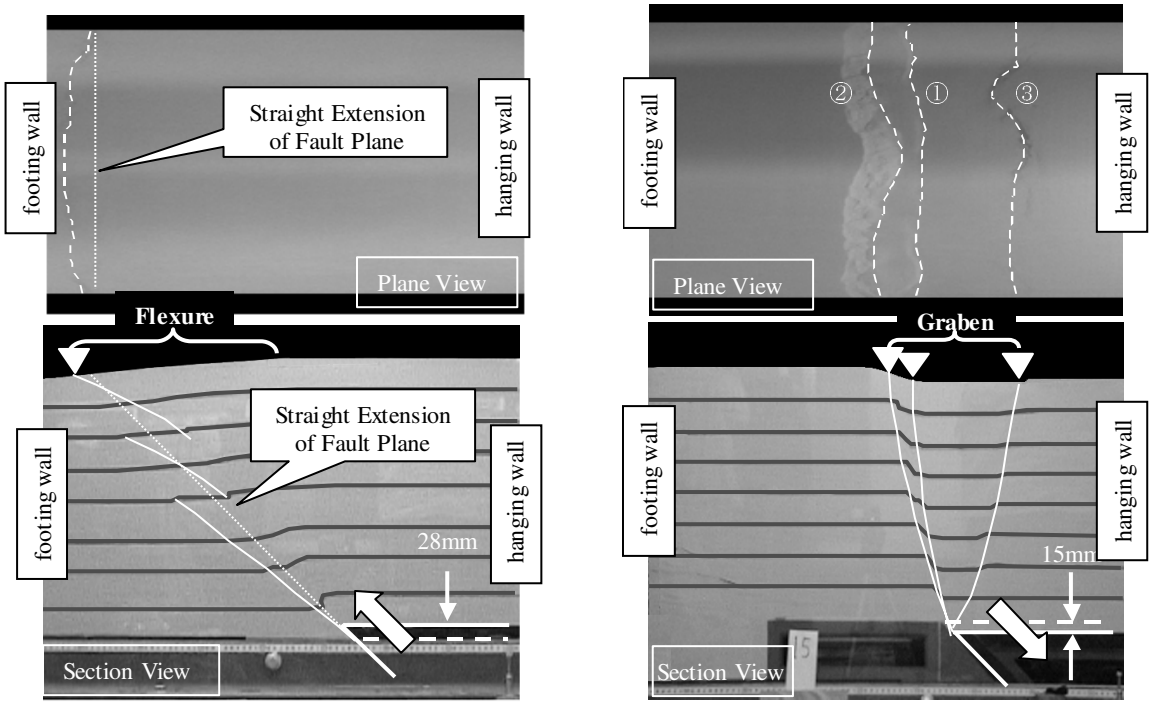

(a) Reverse fault (θ =45°, H=40cm, D=28mm) (b) Normal fault (θ =45°, H=40cm, D=15mm)

Figure 5 Typical rupture pattern for reverse/normal fault

Figure 6 shows the rupture lines on the ground surface for the reverse fault tests. The vertical axis shows the horizontal distance to the locations of the surface ruptures on the ground surface from the bedrock fault, while the horizontal axis is the distance from the each sidewall.

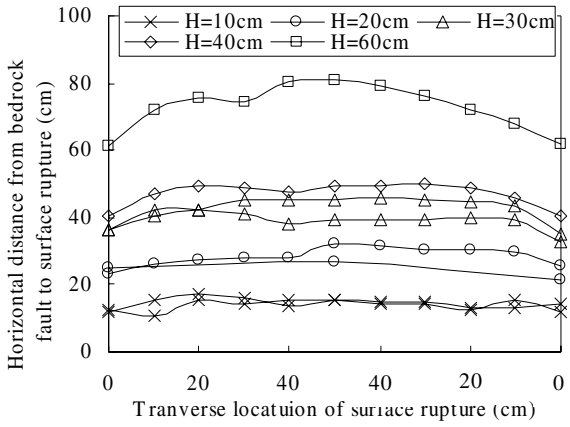

Figure 6 Shape of the surface rupture along the model width with variation of thickness of model

The reduction of the horizontal distance nearby both of the sidewalls shows the effect of the friction between the walls and the model ground. In most of the testing cases besides the one with a thickness of 60cm, the distance is mostly uniform and the effect of the friction can be negligible in the center of the model ground. In the case of the thickness 60cm, there maybe appeared some effects of the friction. However, the difference between the distance at the center of the soil box and the one along either of sidewalls is less than 25%. Thus, for the case with 60cm in its thickness, the locations of surface fault rupture were estimated by taking the average of the measured values with exemption of the two points near each sidewall. On the other hand, the patterns of fault rupture propagation for reverse fault

appeared to vary with a change of dip angle, whereas no explicit alteration of the rupture patterns has been observed regarding the change of dip angle for normal fault. **Figure 7** shows that the observed typical shapes of rupture planes in a sandy soil corresponding to the variations in dip angle of reverse faults.

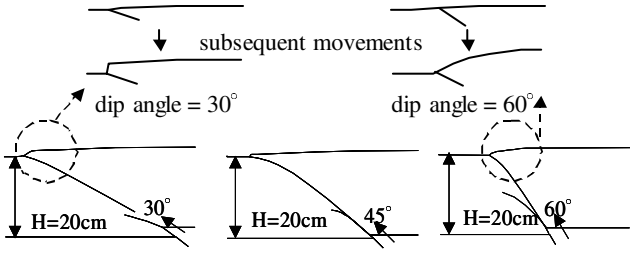

Figure 7 Drawings of rupture shape corresponding to dip angle in reverse faults, H=20cm

The patterns of fault rupture for all three dip angles were seen to be essentially identical with a view point of their characteristic that showed the gradual decrease in dip near the ground surface and the generation of distortion of ground surface appeared prior to the occurrence of scarp on the surface of ground. However, as the dip angle of fault became deeper, i.e. for dip angle=60°, the warping of ground surface near the surface rupture appeared to be significant and subsequent movements on the bedrock fault resulted in deepening the deformation of ground surface. On the contrary to this, for the case with 30° in dip angle, more subsequent fault movements resulted in sliding on the failure plane without further deformation of the ground surface expressed by warping.

Location of Surface Rupture Regarding Dip Angle and Model Thickness

Based on the rupture patterns observed from the testing results as described in the previous section, the key sketch for observation of rupture pattern is depicted as **Figure 8**.

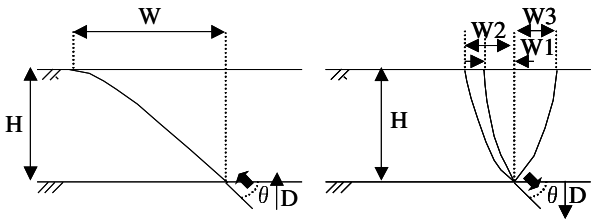

(a) Reverse fault (b) Normal fault

Figure 8 Key sketch for the evaluation of rupture patterns

Referring to the sketch, the relationship between the horizontal distance, W, from the bedrock fault to the location of surface rupture and its factors involving the dip angle θ, the height of the soil mass H, the vertical offset of fault D and the relative density of soil mass D_r, can be explained as shown in **Figure 9**. Those factors can be considered as follows;

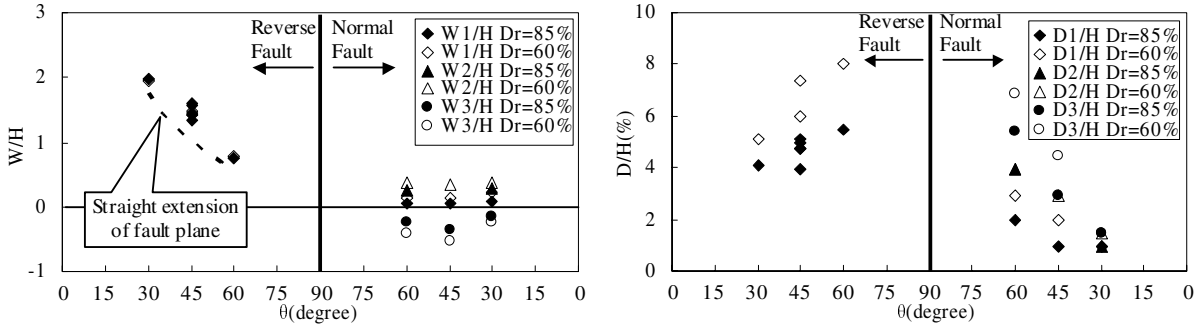

(a) W/H versus θ (b) D/H versus θ

Figure 9 Variation of W/H and D/H as a function of θ and a function of H from 1g test

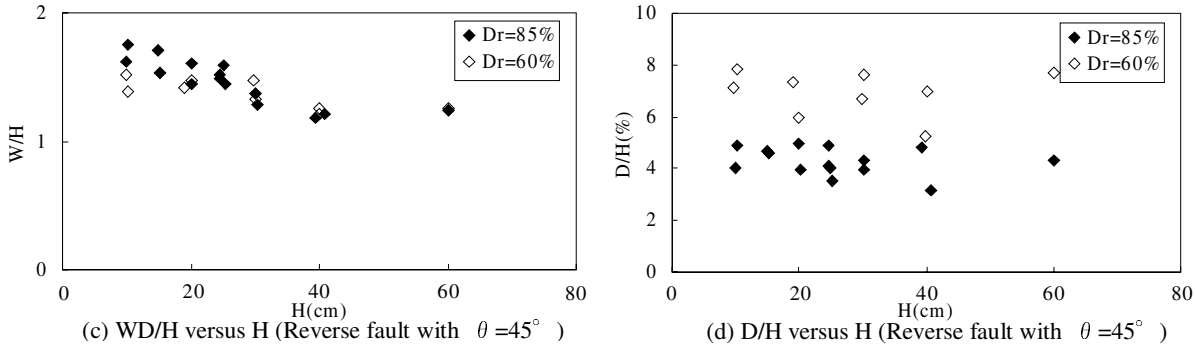

(c) WD/H versus H (Reverse fault with θ =45°) (d) D/H versus H (Reverse fault with θ =45°)

Figure 9 Variation of W/H and D/H as a function of θ and a function of H from 1g test

Relationship between Location of Surface Fault Rupture and Dip Angle

Figure 9 (a) shows the relationship between the normalized distance W/H and the dip angle. For reverse fault, there appeared a definite decrease of the normalized distance of surface fault rupture with increase of the dip angle, however, there is no significant change of W/H for normal fault. And comparison of the locations of the surface rupture with the extension of fault plane as depicted in **Figure 9 (a)** indicates that the reverse faults for all the present dip angles reached to the ground surface farer than the extension of fault plane altogether. Besides, it can be also found for the results with normal fault that the distance between the surface rupture in the hanging wall (W_1 and W_2) and that in the footing wall (W_3) became lager with the looser sand, i.e. D_r=60%. This implies that the graben which means the subsided ground surface bounded by the two rupture planes, W_2 and W_3, may become larger in its width in accordance with the lower relative density of sand.

Relationship Required Vertical Offset and Dip Angle

The variation of D/H according to the changes of dip angle in **Figure 9 (b)** illustrates that the required offset at bedrock to rupture the model surface was seen to be associated to the dip angle. The value of D/H for reverse faults appeared to become greater with increase of the dip angle, whereas the increase of dip angle tended to reduce the required vertical offset for normal faults. The results from the normal fault tests are further showing that the model with small dip angle, θ =30°, produced the rupture lines on the model surface within a small range of D/H saying 1.0~1.5 approximately, whereas the model with large dip angle generated them in a large range of D/H from 1.9 to 6.8. This means that the normal fault with a small dip angle is apt to form a graben at a relatively small amount of vertical offset at bedrock.

Relationship Location of Surface Fault Rupture and Model Thickness

Figure 9 (c) shows a slight decrease of W/H with increase of the model thickness that means the distance between the surface fault rupture and the bedrock fault (W) is apparently associated with the model thickness. This implies that the rupture pattern could change as the thickness of the soil mass is varied under the low confining pressures under which the experiments were conducted in this study, i.e. the corresponding confining pressures ranged from approximately 1.5KPa to 4.0KPa. Besides, this result demonstrates a different tendency from the previous study conducted by Tani et al. [3] that showed little change of the location of surface fault as the model thickness is varied. However, it is certainly expected that the dry sands used in both of the studies performed by Tani et al. [3] and the authors can exhibit strongly volume change tendency during their shearing deformation under the extremely low confining pressures corresponding to their 1-g models, which may bring about a change of rupture pattern according to the model thickness. This fact accordingly invoked the employment of centrifuge test to the physical model in this study to investigate the fault rupture propagation under high confining pressure condition. This aspect of soil response is further discussed with the centrifuge test results in this study.

Relationship Required Vertical Offset and Model Thickness

It can be seen in **Fig. 9 (d)** that the value of D/H was seen as mostly uniform with reference to the model thickness for both the looser and denser sands. The results with reverse faulting further show that the fault ruptures reached to the ground surface in the sand with D_r=85% at the normalized vertical offset of approximately 3.3~4.8%, while in the sand with D_r=60%, the surface fault ruptures initially occurred at the normalized vertical offset of approximately 6.0~7.7%, which indicates that more vertical offset should be given to the looser sand to rupture the ground surface.

On the contrary, as shown in **Figure 9 (b)**, for the normal faults, the rupture planes in the tests with normal fault initially formed over the entire model thickness at the less normalized vertical bedrock fault displacement (D_1/H, denoted by ◇, ◆ in the figure) of 1.0~3.0% compared with those from the reverse faults tests, which have shown that the normal faults may not be so much affected by the relative densities of soil as the reverse faults.

These results are fairly consistent with those reported by Cole at al. [1] who found that a complete slip surface formed in a 45 ㎝ high test model composed of a dense dry sand at a normalized vertical bed rock fault displacement of 1~ 3.3% with normal faults and 2~4.5% with reverse faults.

Width of Distorted Surface Regarding Dip Angle and Model Thickness

The width of flexure and graben was also assessed with respect to the dip angle and the model thickness. All the widths herein were measured at the moment that the fault rupture reached to the ground surface during the fault box tests. Based on the rupture patterns observed from the experiments, the key sketch for the width of flexure and graben is depicted as **Figure 10**.

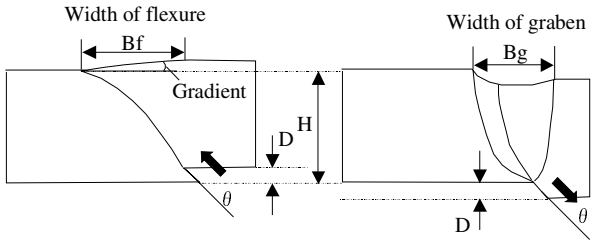

Figure 10 Key sketch for the evaluation of width of flexure and graben

Relationship between Width of Flexure and Graben and Dip Angle

Figure 11 shows that the widths of flexure resulted from the reverse fault were observed to vary depending upon the dip angle in such a way that the fault movement with a relatively low dip angle produces the large width of flexure. On the contrary, the widths of graben resulted from the normal faults revealed no apparent variation with the change of dip angle. It may be also inferred from **Figure 11** that the reverse faults with a shallow dip angle tend to create the deformation of surface ground expressed by warping in a wider range than those with a deep dip angle as the rupture plane propagates up through the ground model. Besides, the width of flexure and graben that the looser sand appeared to produce larger widths of flexure and graben than the denser sand.

Figure 12 illustrates the relationship between the gradient of flexure and the dip angle. The gradient of flexure appeared to become gradually larger for the greater value of dip angle as shown in **Figure 12**.

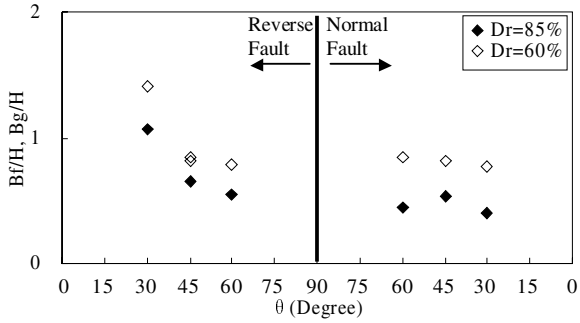

Figure 11 Width of flexure and graben versus dip angle

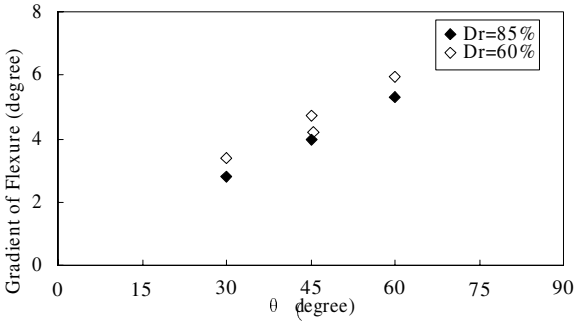

Figure 12 Gradient of flexure versus dip angle

Meanwhile, **Figure 12** also shows that the gradients of flexure in the looser sand (D_r=60%) appeared to be slightly greater than those in the denser sand (D_r=85%). The greater values of the widths of flexure and graben and the gradient of flexure for the looser sands may indicate that the deformation of ground surface resulting in the flexure took place more significantly at the looser sands as the rupture appeared on the ground surface. It could be due to the relatively large amount of bedrock displacement to rupture the ground surface, which is attributed to the some high ductility of the looser sand compared to the denser sand. In brief, the looser sand could absorb the differential displacements of the underlying fault locally without yielding a distinct rupture on the model surface.

Relationship between Width of Flexure and Model Thickness

Figure 13 shows that the ratios of width of flexure to model thickness appeared to be mostly constant to the change of model thickness. At the same time, the looser sands appeared to produce slightly larger widths of flexure than the denser sand as shown in **Figure 13**.

Besides, as shown in **Figure 14**, the gradients of flexure also appeared to be independent of the change of model thickness.

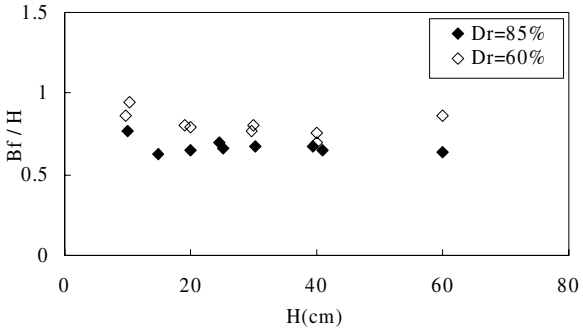

Figure 13 Width of flexure versus model thickness

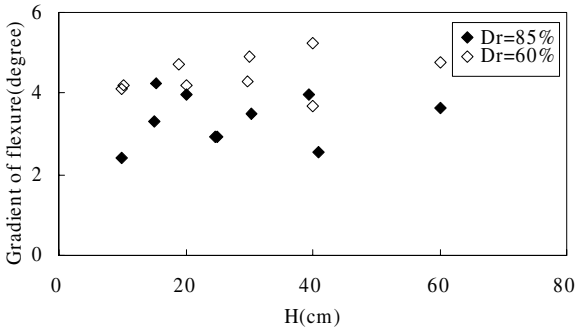

Figure 14 Gradient of flexure versus model thickness

These results implies that the deformation of ground surface induced by fault movements at the specific vertical offset at bedrock that can bring about a surface fault rupture may be affected mainly by the dip angle and the ductility of soil rather than the model thickness.

OBSERVED BEHAVIOR FROM CENTRIFUGE MODEL TESTS

A series of centrifuge tests was carried out to investigate the effect of various confining stresses on the propagation of fault rupture through a sand deposit. The pattern of fault ruptures and the location of surface rupture caused by reverse fault in a sand deposit was mainly examined through the models having various thickness which can be achieved by applying different levels of gravity to each prototype model.

Rupture Pattern from Centrifuge Model Faulting Tests

The overall features of fault rupture propagation through the four different sand layers of which physical thickness and centrifugal gravities are changing are shown in **Figure 15**. These features also exhibited the same nature with those in 1-g tests by showing the decrease in dip near the ground surface.

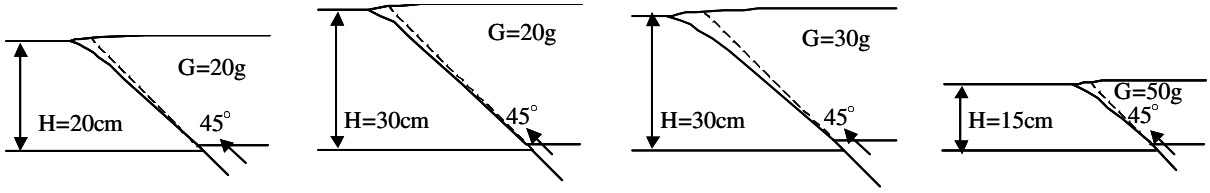

Figure 15 Sketch of rupture shape corresponding to each case under centrifuge condition

However, while the plural number of failure planes was well observable at any cases thicker than 20 cm in the model thickness from the 1-g fault box tests as shown in **Figure 5 (a)**, such type of failures

that showing a few of broken lines was not obviously visible with the centrifuge models. The centrifuge models yielded a rupture plane over the entire thickness of model. Furthermore, as shown in **Figure 15**, the rupture patterns in the centrifuge models appeared to be mostly identical for all cases under the stress condition during the tests in spite of the change of model thickness. Now that the difference between the 1-g models and the centrifuge models is nothing but the level of confining stress, it can be said that the patterns of rupture propagation through the sand deposit can change depending upon the stress levels.

Figure 16 shows the rupture lines on the ground surface for the centrifuge fault tests in the same way to **Figure 6** obtained from the 1-g models. Similar to the results form the 1-g models, even though the reduction of the horizontal distance nearby the sidewalls was shown due to the friction between the walls and the model ground, the distance is mostly uniform and the effect of the friction can be negligible in the center of the model ground in most of the testing cases.

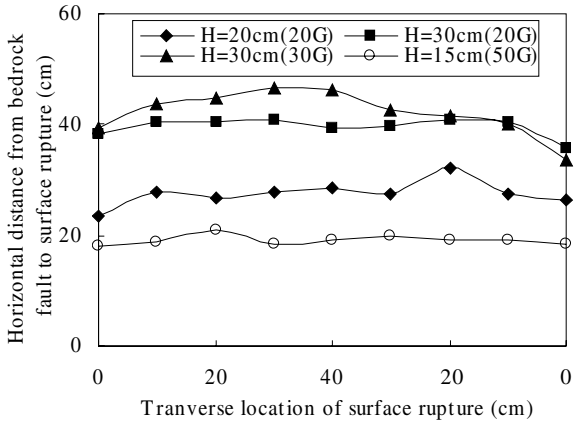

Figure 16 Profile of ground surface exposed to reverse fault movement under centrifuge condition

Verification for Effect of Model Thickness

Location of surface fault rupture with increased model thickness

Figure 17 shows the variation of the distance from the bedrock fault to the surface rupture normalized by the model thickness with respect to the model thickness. The model thickness in the horizontal axis of the figure means the equivalent thickness of model which can be acquired by applying different gravitational acceleration to the thickness of each prototype model. It can be noticed from **Figure 17** that the ratio of W/H appeared to be mostly uniform without showing any definite tendency relating to the variation of model thickness.

Considering the finding from the 1-g models that demonstrated the declining tendency of W/H with increase of the model thickness as shown in **Figure 9 (c)**, this result indicates that given the stress levels corresponding to the centrifuge models, the pattern of rupture propagation which is subjected to determine the location surface rupture (indicated by the distance W in **Figure 8**) did not exhibit significant variation according to the change of model thickness. Hence it can be said that the prediction of fault rupture propagation using the physical models under extremely low stress conditions should be carefully interpreted to avoid the inaccuracy due to the changing pattern of rupture propagation according to the model thickness.

Required offset with increased model thickness

It can be seen form **Figure 18** that the ratios of D/H are also independent of the model thickness, which is the same trend as those in 1-g models as plotted in **Figure 9 (d)**. But the value of D/H in the centrifuge models occurred as a little greater than those in the 1-g models at the specific density of 85% for the sand used in the tests.

Width of flexure with increased model thickness

Figure 19 shows the ratio of width of flexure to model thickness corresponding to variation of the model thickness in the centrifuge models. The results show the uniform value of the ratio B_f/H with respect to the model thickness, which is the same trend as those in 1-g models as shown in **Figure 13**.

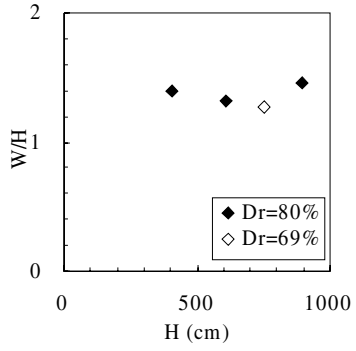

Figure 17 W/H versus model thickness from centrifuge model

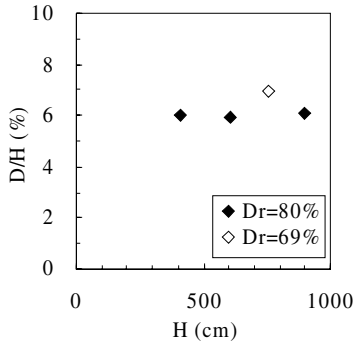

Figure 18 D/H versus model thickness from centrifuge model

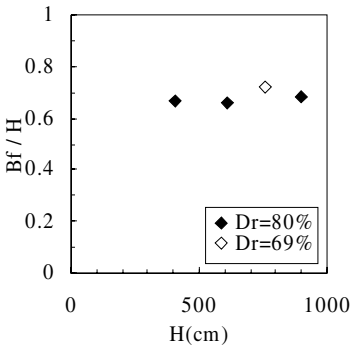

Figure 19 D/H versus model thickness from centrifuge model

Shearing Behavior of Sandy Soil during fault rupture under various stress levels

As addressed previously, the two series of reverse fault tests at 1-g and centrifuge conditions provided us an observable finding presenting the change in the location of surface fault in accordance with confining stresses, which means the patterns of rupture propagation vary depending upon the stress levels. This stress dependent characteristic of fault rupture propagation can be understood by taking a careful look into what the dominant factor is to control the development of shear rupture zones within a sandy soil overlying the bedrock fault. Some researchers found that the dominant factor controlling velocity characteristics and direction of localized shearing deformation concerning the sandy soil subjected to fault movement is the angle of dilation for the soil (Cole et al. [1], Stone et al. [6]). Moreover, it can be well expected that the granular material as like the sand used in this study tends to exhibit strongly dilatant behavior at low confining stress.

Observed Shearing Behavior of Sand under Extremely Low Confining Stresses

Stone et al. [6] provided an experimental result through a series of faulting tests and rotating wall tests showing an abrupt transformation of localized shearing deformation - discontinuity formation - within a granular soil mass subjected to continuous boundary movements that was owing to the change of the dilation angle for the soil during process of shearing deformation. This phenomenon can be also obviously observed in the author's experiments by monitoring the propagation of fault ruptures within the ground model of lager thickness among the testing cases under 1-g condition as illustrated in **Figure 20**.

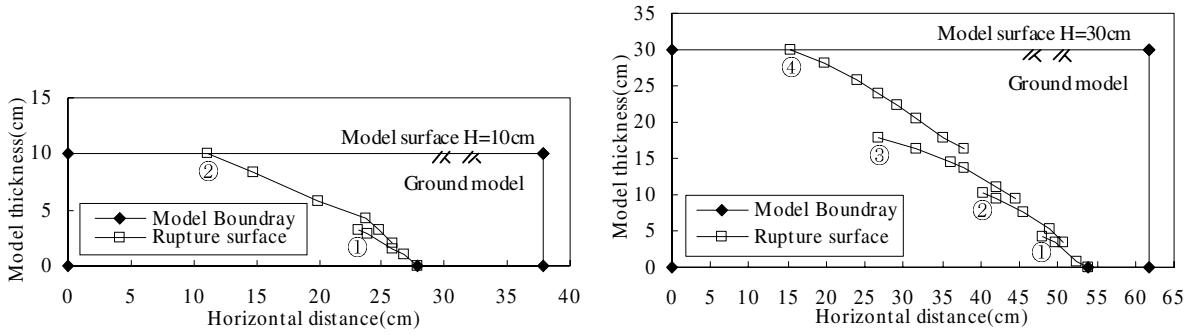

(a) Model thickness=10cm

(b) Model thickness=30cm

Figure 20 Multiple failure surfaces observed in 1-g models

As the movable base of testing box moved up and into the soil mass in the same direction of fault plane, the initial localized shearing region denoted by Number ① in **Figure 20** first took place and propagated upward to the surface ground and away from the extension of fault plane, but subsequent movements of the base produced a new localization of shearing denoted by Number ② above the

existing localized region and then repeated the same procedure until it reached to the free surface of ground model. Once the new localization occurred, movement on the previous localization ceased. This aspect of soil response had generated even more than four localized shearing regions with the thicker ground models. This plural form of shearing surfaces with higher thickness of model was well introduced at the similar tests performed by Ueta et al [4] as well. However, the lower the thickness of model is, the smaller the number of localized deformation is definitely. As shown in **Figure 20 (a),** for the failure for the lower models (H<20㎝), the secondary localized shearing region continuously propagated to the surface with a single localization (some of the thinner models yielded single localization).
Furthermore, as the localization is newly generated by progress of the fault movement, it can be seen that its advancing direction angle tends to be deliberately smaller with respect to the direction of fault plane, as shown in **Figure 21**.

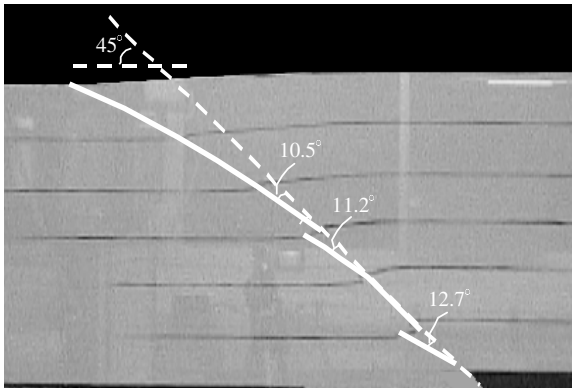

Figure 21 Direction angles of shear failure plane

This implies that relatively large displacement in higher thickness of models required to rupture the model surface caused greater change of the dilation angle during the course of tests so that the initial surface failure could encounter kinematic incompatibility and might create a new localized shear region. Hence, provided that a significant value of dilation angle and its rapid variation during shearing process for a isotropic dry sand at extremely low confining pressure are validly expected, it can be understood reasonably that the shear zone patterns in the soil change with a definite tendency at the stress levels under which the 1-g tests were implemented.

Observed Shearing Behavior of Sand with Increase of Confining Stresses
In the mean time, as for the centrifuge tests, although the shape of failure surface is similar to that observed in the results of 1-g tests, there were not so much apparent transformation of localized shearing region as that discovered at the models of higher thickness among the 1-g tests, which is consistent with all of the centrifuge tests as shown in **Figure 22**.

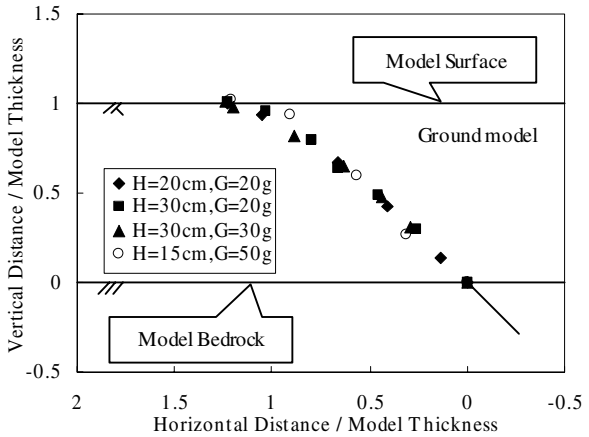

Figure 22 Identical rupture patterns in centrifuge models

This result indicates that the volume change tendency of the sand under centrifuge condition little varies owing to the increase of confining pressure. Moreover, the dilation angle of the sand itself will be lessened according to increase of the stress level.(Stone et al. [6], Bolton [7])
In brief this character of granular soil may be able to make the singular rupture pattern regardless of change of model thickness under high confining pressure, whereas it causes the individual rupture pattern as to model thickness under extremely low confining pressure, so that the location of surface rupture may be changed depending upon the different rupture pattern regarding the model thickness.
In the long run, the centrifuge model could provide more stable prediction of the location of surface rupture, which quite better represents the response of prototype material.

CONCLUSION

The patterns and the location of fault rupture in a sandy soil deposit overlying active dip-slip fault have been studied on the basis of the results from 1-g and centrifuge fault box tests. The relationship of the location of surface rupture and its affecting factors such as the type of faults, the density of soil and the dip angle of fault plane were evaluated. At the same time, the extents of flexure and graben accompanied by the surface fault ruptures were also investigated. Two different patterns of fault rupture propagation according to the faulting type(normal /reverse fault) within a sandy soil deposit can be identified in a similar manner formerly provided by the small model tests (Cole et al. [1], Tani et al. [3]). It is also founded changing the angle of fault plane with reverse fault could greatly affect the location of surface fault rupture. But unlike the findings from the similar studies, the 1-g model tests with change of the model thickness indicated that the location of surface rupture might be definitely influenced by the change of model thickness at low confining pressure. By comparison with the results from centrifuge models, it can be inferred that the soil behavior at the 1-g model tests is owing to remarkable volume change tendency of a dry sand under corresponding stress level to the 1-g models.
Consequently it is confirmed from this study that the physical models at 1-g condition for fault rupture propagation might provide a properly simulating method to approximately understand the response of sandy soil over the various types of bedrock fault movement. However, for further understanding of the phenomenon to consider a mitigation method against hazards in real fields, an adequate centrifuge model should be taken into reproduction of fault rupture propagation to predict that behavior as close to real phenomenon as possible.

ACKNOLEDGMENTS

The authors wish to thank the great dedication of Dr. T. Matsuda and his staffs in Dynamics Research Center of Obayashi Cooperation, Tokyo, Japan to the centrifugal model tests on this subject**.**

REFERENCES

1. Cole, D. A., Jr., and Lade, P. V., Influence zones in alluvium over dip-slip faults, *Journal of Geotechnical Engineering*, ASCE, Vol. 110, No. GT5, pp. 599-615, 1984
2. Bray, J. D., Seed, R. B., and Seed, H. B., Analysis of earthquake fault rupture propagation through cohesive soil, *Journal of Geotechnical Engineering,* ASCE, Vol. 120, No 3., pp. 562-580, 1994
3. Tani, K., Ueta, K. and Onizuka, N., Scale effect of quaternary ground deformation observed in model tests of vertical fault, *Proceeding of 29th Japan National Conference on SMFE*, pp. 1359~1362, 1994 (in Japanese)
4. Ueta, K. and Tani, K., Deformation of quaternary deposits and ground surface caused by bedrock fault movements (Part 2) -Normal and reverse fault model tests-, *Abiko Research Laboratory Rep. No. U98048*, 1999 (in Japanese)
5. Roth, W. H., Scott, R. F. and Austin, I., Centrifuge modeling of fault propagation through alluvial soils, *Geophysical Research Letters*, Vol. 8, No. 6, pp. 561-564, 1981
6. Stone, K. J. L. and Wood, D.M., Effects of dilatancy and particle size observed in model tests on sand, *Soils and Foundations*, JSSMFE, Vol. 32, No 4., pp. 43-57, 1992
7. Bolton, M. D., The strength and dilatancy of sands, *Geotechnique* 36, No. 1, pp. 65-78, 1986
8. Johansson, J. and Konagai, K., Fault surface rupture experiments: a comparison of dry and saturated soils, *Proceeding of 27th Symposium on Earthquake Engineering*, JSCE, paper No. 271, 2004.
9. Lee, J. W., Iwanaga, R, Tabuchi, G. and Hamada, M., An experimental study on fault rupture propagation in sandy soil deposit, *Proceeding of 4th Symposium on Enhancement of Earthquake Performance of Infrastructure Based on Investigation into Fracture Progress,* JSCE, pp. 265~270, 2003